Inorganica Chimica Acta, *189* (1991) 175–187

Synthesis, chemical and electrochemical deprotonation reactions of aminocarbene complexes of palladium(II) and platinum(II). X-ray structure of $\{(PPh_3)ClPt[\mu\text{-}\overline{COCH_2CH_2N}\text{-}C,N]\}_2$

Roberta Bertani, Mirto Mozzon, Rino A. Michelin*
Centro di Chimica e Tecnologia dei Composti Metallorganici degli Elementi di Transizione del CNR and Istituto di Chimica Industriale, Facoltà di Ingegneria, Università di Padova, via F. Marzolo 9, 35131 Padua (Italy)

Franco Benetollo
Istituto di Chimica e Tecnologia dei Radioelementi del CNR, Corso Stati Uniti 4, 35020 Padua (Italy)

Gabriella Bombieri
Istituto di Chimica Farmaceutica, Università di Milano, viale Abruzzi 42, 20131 Milan (Italy)

Tania J. Castilho and Armando J. L. Pombeiro*
Centro de Quimica Estrutural, Complexo I, Instituto Superior Tecnico, Av. Rovisco Pais, 1096 Lisbon Codex (Portugal)

(Received June 13, 1991)

Abstract

The diaminocarbene complexes *cis*-$Cl_2(PPh_3)Pt[\overline{CN(Bu^t)CH_2CH_2NH}]$ (**1**) and *cis*-$Cl_2Pt[\overline{CN(C_6H_4\text{-}p\text{-}OMe)CH_2CH_2NH}]_2$ (**2**) have been prepared by reaction of the corresponding isocyanide derivatives with aziridine/$ClCH_2CH_2NH_3^+Cl^-$ and aziridine alone, respectively. The aminooxycarbene complex *cis*-$Cl_2Pt[\overline{CN(C_6H_4\text{-}p\text{-}OMe)CH_2CH_2O}]_2$ (**3**) has been prepared by reaction of the bis-isocyanide derivative with 2-chloroethanol/n-BuLi. The dimeric complexes $\{(PPh_3)BrPd[\mu\text{-}\overline{CN(Me)CH_2CH_2N}\text{-}C,N]\}_2$ (**4**), $\{(PPh_3)ClPd[\mu\text{-}\overline{CN(C_6H_4\text{-}p\text{-}OMe)CH_2CH_2N}\text{-}C,N]\}_2$ (**5**), $\{(PPh_3)ClPt[\mu\text{-}\overline{CN(C_6H_4\text{-}p\text{-}OMe)CH_2CH_2N}\text{-}C,N]\}_2$ (**6**) have been prepared by deprotonation reaction of the NH group of the corresponding mononuclear derivatives with n-BuLi. The X-ray structure of $\{(PPh_3)ClPt[\mu\text{-}\overline{COCH_2CH_2N}\text{-}C,N]\}_2$ (**7**) is reported. The structural model was refined to $R=0.055$ ($R_w=0.061$) for 7442 independent reflections. Crystal data: triclinic, space group $P\bar{1}$, $a=19.564(3)$, $b=16.497(3)$, $c=13.243(2)$ Å, $\alpha=88.93(3)$, $\beta=97.88(3)$, $\gamma=91.97(3)°$, $Z=4$. The crystal contains two crystallographically independent dimer units and a disordered dichloroethane molecule. Each dimer is formed by two bridging carbene ligands which are coordinated to one platinum on one side via a Pt–N bond and to the second platinum via a Pt–C bond. The coordination geometry around each platinum atom is an irregular square with deviations in the tetrahedral direction of the bonded atoms. The anodic behaviour of these and related monocarbene, dicarbene or dinuclear dicarbene complexes has been studied by cyclic voltammetry and controlled potential electrolysis in aprotic media and shown to present irreversible oxidation waves commonly with a multi-electron character (up to four electrons) and involving liberation of protons (in a number similar to that of the transfered electrons) conceivably resulting from anodically induced N–H or C–H bond cleavage, the former at an amino group and the latter occurring at methylene groups activated by adjacent amino- or oxy-carbene moieties.

Introduction

We have recently reported that one or even two RNC ligands in Pt(II) and Pd(II) complexes can be converted in high yield to the corresponding five-membered cyclic diaminocarbene derivatives [1]. The N–H group in cationic complexes of the type *trans*-$\{(PPh_3)_2M[\overline{CN(C_6H_4\text{-}p\text{-}X)CH_2CH_2NH}]Br\}^+$ ($M=Pd$, Pt; $X=Me$, OMe) can be deprotonated by n-BuLi to give the corresponding imino intermediate which rapidly reacts with electrophiles R–X ($R=CH_2CH{=}CH_2$, $CH_2\text{–}C{\equiv}CH$; $X=Br$) to give new functionalized N–R carbenes [1]. Also amino-oxy-carbene compounds like $Cp(CO)_2Fe(\overline{COCH_2CH_2NH})^+$ [2a, b] or $Re(CO)_4(Br)(\overline{COCH_2CH_2NH})$ [2c] were reported to react with strong bases to yield the corresponding neutral imino complexes. Generally, n-BuLi has been used as the base

---

*Authors to whom correspondence should be addressed.

0020-1693/91/$3.50

for the reported deprotonation reactions of the N–H group, other bases like NEt_3, $LiAlH_4$ or $NaN(SiMe_3)_2$ having proved unsuccessfull [2, 3]. The present work will focus on (i) synthetic investigation and structural properties of dimeric Pt(II) and Pd(II) complexes having bridging carbene ligands derived from deprotonation reactions of neutral monomeric aminocarbene complexes such as *cis*-$Cl_2(PPh_3)M[\overline{CN(C_6H_4\text{-}p\text{-}OMe)CH_2CH_2NH}]$ (M = Pd, Pt) with n-BuLi and (ii) electrochemical anodic behavior of neutral aminocarbene complexes. As for the latter aspect, despite the extensive developed chemistry of complexes with multiple metal–carbon bonds [4–6], only a small number of electrochemical studies of these species has been reported [7–14]. We have previously outlined [14] the redox behavior of some rhenium phosphine complexes with a variety of multiple metal carbon bonded ligands, particularly amino-carbyne-type complexes derived from protic attack at ligating isocyanides. The results were interpreted in terms of anodically-induced β-dehydrogenation to give the corresponding parent unprotonated complexes.

Experimental

General procedures

All reactions were carried out under a nitrogen atmosphere. Tetrahydrofuran (THF) was distilled from sodium/benzophenone. All other solvents were of reagent grade and used without further purification. IR spectra were taken on a Perkin–Elmer 983 spectrophotometer. ^1H NMR spectra were recorded on a Bruker AM-400 spectrometer. ^{31}P NMR spectra at 32 MHz were recorded on a Varian FT 80A spectrometer. The fast atom bombardment (FAB) mass spectra were obtained on a VG ZAB 2F instrument operating with a Xe-atom beam energy of 8 keV. The elemental analyses were performed by the Department of Inorganic, Organometallic and Analytical Chemistry of the University of Padua. The melting points were taken on a hot plate apparatus and are uncorrected.

Electrochemistry

The electrochemical experiments were carried out either on an EG&G PAR 173 potentiostat/galvanostat and an EG&G PARC 175 Universal programmer or on an HI-TEK DT 2101 potentiostat/galvanostat and an HI-TEK PP RI waveform generator. Cyclic voltammetry was undertaken in a two-compartment three-electrode cell, at a platinum-wire working electrode, probed by a Luggin capillary connected to a silver-wire pseudo-reference electrode; a platinum or tungsten auxiliary electrode was employed. Controlled-potential electrolyses were carried out in a three-electrode H-type cell with a platinum-gauze working and counter electrodes in compartments separated by a glass frit; a Luggin capillary, probing the working electrode, was connected to a silver-wire pseudo-reference electrode. The oxidation potentials of the complexes were measured by cyclic voltammetry in 0.2 mol dm^{-3} $[NBu_4][BF_4]$/NCMe (or CH_2Cl_2 for 7) and the E_p^{ox} values are quoted relative to the SCE by using as internal reference the $[Fe(\eta^5\text{-}C_5H_5)_2]^{0/+}$ couple ($E_{1/2}^{ox}$ = 0.42 or 0.545 V versus SCE, in 0.2 mol dm^{-3} $[NBu_4][BF_4]$/NCMe or CH_2Cl_2, respectively).

The acid-base titrations of the electrochemically oxidized solutions were carried out as indicated in the literature [15], by using a solution of NaOH in CH_3OH which was standardized by titration against benzoic acid in NCMe (thymol blue was used as the indicator). The results presented have been corrected for background effects by performing also, in each case, the titration of the blank solution of 0.2 mol dm^{-3} $[NBu_4][BF_4]$ which has been electrolyzed under identical conditions to those used for the corresponding complex solution.

Moreover, prior to the addition of the complex, each electrolyte solution was pre-electrolyzed at the appropriate potential until a constant and close to zero current, thus conceivably eliminating the interference of eventual traces of residual moisture during the subsequent controlled-potential electrolysis of the complex solution.

Starting complexes

The complexes *cis*-$Cl_2Pd(PPh_3)[\overline{CN(R)CH_2CH_2NH}]$ (R = Bu^t, C_6H_4-*p*-OMe [16]); *cis*-$Cl_2(CNBu^t)Pd[\overline{CN(Bu^t)CH_2CH_2NH}]$ [16]; *cis*-$Br_2(PPh_3)Pd[\overline{CN(Me)CH_2CH_2NH}]$ [1a]; *cis*-$Cl_2(PPh_3)Pt[\overline{CN(C_6H_4\text{-}p\text{-}OMe)CH_2CH_2NH}]$ [16] were prepared according to published procedures.

Synthesis of carbene complexes

Synthesis of cis-$Cl_2(PPh_3)Pt[\overline{CN(Bu^t)CH_2CH_2NH}]$ (1)

A suspension of *cis*-$Cl_2(PPh_3)Pt(CNBu^t)$* (0.263 g, 0.43 mmol) was treated with aziridine (0.086 ml, 1.72 mmol) and $ClCH_2CH_2NH_3^+Cl^-$ (0.060 g, 0.52 mmol) in THF (30 ml) at 0 °C. Then, the reaction mixture was warmed to room temperature and stirred for 48 h. The white precipitate formed was filtered

---

**cis*-$Cl_2(PPh_3)Pt(CNBu^t)$ was prepared as reported [16] for the analogous Pd(II) compound. IR: ν(CN) 2230 s, ν(PtCl) 300 m, 333 m, cm^{-1}; ^1H NMR (CD_2Cl_2): $\delta(Bu^t)$ 1.12 s; ^{31}P NMR (CD_2Cl_2): δ(P) 8.17 s, $^1J(Pt\text{–}P)$ 3406 Hz.

off, washed with MeOH (3 × 10 ml), n-hexane (3 × 10 ml) and dried under vacuum. Yield 0.200 g (71%); m.p. 284–285 °C. *Anal.* Calc. for $C_{25}H_{29}N_2Cl_2PPt$: C, 45.88; H, 4.46; N, 4.28. Found: C, 45.26; H, 4.50; N, 4.15%.

Synthesis of $cis\text{-}Cl_2Pt[\overline{CN(C_6H_4\text{-}p\text{-}OMe)\text{-}CH_2CH_2NH}]_2$ *(2)*

A solution of *cis*-$Cl_2Pt(CNC_6H_4\text{-}p\text{-}OMe)_2$ [1b] (0.513 g, 0.96 mmol) in THF (50 ml) at 0 °C was treated with aziridine (0.15 ml, 3.00 mmol). After 1 h the reaction mixture was warmed to room temperature. IR spectra of the solution taken periodically showed the appearance of the C=N band at 1506 cm^{-1} of the final product and the progressive disappearance of the C≡N band at 2191 cm^{-1} of the starting isocyanide complex. After 2 h a white precipitate was formed, but the reaction mixture was stirred for an additional 24 h. Then the solid was filtered, washed with n-hexane (3 × 10 ml) and dried under vacuum. Yield 0.450 g (75%); m.p. 226–228 °C. *Anal.* Calc. for $C_{20}H_{24}N_4Cl_2O_2Pt$: C, 38.84; H, 3.91; N, 9.06. Found: C, 38.60; H, 4.07; N, 9.15%. FAB mass spectrum: *m*/*e*, 618 $[M]^+$; 583, $[M-Cl]^{+\cdot}$; 548, $[M\text{-}2Cl]^+$; 533, $[M\text{-}2Cl\text{-}CH_3]^{+\cdot}$; 502, $[M\text{-}2Cl\text{-}CH_3\text{-}CO]^{+\cdot}$.

Synthesis of $cis\text{-}Cl_2Pt[\overline{CN(C_6H_4\text{-}p\text{-}OMe)\text{-}CH_2CH_2O}]_2$ *(3)*

To a solution of $ClCH_2CH_2OH$ (1 ml, 14.92 mmol) in THF (50 ml) at 0 °C was added a 1.5 M solution in n-hexane of n-BuLi (1.37 ml, 2.07 mmol). After a few minutes *cis*-$Cl_2Pt(CNC_6H_4\text{-}p\text{-}OMe)_2$ (0.50 g, 0.94 mmol) was added and the reaction mixture was stirred at 0 °C for 15 min and then allowed to reach room temperature. An IR spectrum of the reacting solution showed the presence of the C=N band at 1512 cm^{-1} and did not reveal any C≡N stretching of the starting complex. After 1 h a white precipitate was formed. The mixture was taken to dryness under reduced pressure and the solid was washed with MeOH (2 × 10 ml), CH_2Cl_2 (2 × 10 ml) and Et_2O (2 × 10 ml) and dried under vacuum. Yield 0.48 g (83%); m.p. 185–186 °C. *Anal.* Calc. for $C_{20}H_{22}N_2Cl_2O_4Pt$: C, 38.72; H, 3.57; N, 4.51. Found: C, 39.09; H, 3.75; N, 4.62%. FAB mass spectrum: *m*/*e*: 620, $[M]^+$; 585, $[M-Cl]^+$; 550, $[M\text{-}2Cl]^+$; 373, $[Pt\overline{CN(C_6H_4OCH_3)CH_2CH_2O}]^{+\cdot}$.

Reactions with n-BuLi

Synthesis of $\{(PPh_3)BrPd[\mu\text{-}\overline{CN(Me)\text{-}CH_2CH_2N}\text{-}C,N]\}_2$ *(4)*

A suspension of *cis*-$Br_2(PPh_3)Pd[\overline{CN(Me)\text{-}CH_2CH_2NH}]$ [1a] (0.152 g, 0.29 mmol) in THF (50 ml) was treated with a 1.5 M n-hexane solution of n-BuLi (0.19 ml, 0.29 mmol) at 0 °C. The reaction mixture was stirred at 0 °C for 1 h and then at room temperature for 4 h. The solution was taken to dryness, treated with CH_2Cl_2 (20 ml), filtered and concentrated to small volume (3 ml). On addition of n-hexane (10 ml) a white solid precipitated. The precipitate was filtered, washed with n-hexane (3 × 10 ml) and dried under vacuum. Yield 0.110 g (72%); m.p. 210–212 °C. *Anal.* Calc. for $C_{44}H_{44}N_4Br_2P_2Pd_2$: C, 49.70; H, 4.16; N, 5.27. Found: C, 49.20; H, 4.07; N, 5.17%. FAB mass spectrum: *m*/*e*: 530, $[(PPh_3)BrPd(\overline{CNMeCH_2CH_2N})]^{+\cdot}$.

Synthesis of $\{(PPh_3)ClPd[\mu\text{-}\overline{CN(C_6H_4\text{-}p\text{-}OMe)\text{-}CH_2CH_2N}\text{-}C,N]\}_2$ *(5)*

A suspension of *cis*-$Cl_2(PPh_3)Pd[\overline{CN(C_6H_4\text{-}p\text{-}OMe)CH_2CH_2NH}]$ [16] (0.250 g, 0.41 mmol) in THF (50 ml), was treated with n-BuLi (0.44 mmol, 0.28 ml of a 1.6 M n-hexane solution) at 0 °C. After 5 min the reaction mixture changed from white to yellow and was stirred at 0 °C for 15 min and then at room temperature for 1 h. The solution obtained was taken to dryness, washed with MeOH (3 × 5 ml), n-hexane (2 × 5 ml) and dried under vacuum. Yield 0.196 g (84%); m.p. 276–278 °C. *Anal.* Calc. for $C_{56}H_{52}N_4Cl_2P_2O_2Pd_2$: C, 58.05; H, 4.52; N, 4.83. Found: C, 57.93; H, 4.66; N, 4.76%. FAB mass spectrum, *m*/*e*: 578, $[(PPh_3)ClPd(\overline{CN(C_6H_4\text{-}p\text{-}OMe)CH_2CH_2N})]^+$; 543, $[M/2-Cl]^{+\cdot}$.

Synthesis of $\{(PPh_3)ClPt[\mu\text{-}\overline{CN(C_6H_4\text{-}p\text{-}OMe)\text{-}CH_2CH_2N}\text{-}C,N]\}_2$ *(6)*

The reaction was performed in a manner similar to that reported for 4 starting from *cis*-$Cl_2(PPh_3)Pt[\overline{CN(C_6H_4\text{-}p\text{-}OMe)CH_2CH_2NH}]$ [16] (0.246 g, 0.35 mmol) and n-BuLi (0.52 mmol, 0.33

TABLE 1. Crystallographic data

Chemical formula	$[Cl_2Pt_2(PPh_3)_2(\overline{COCH_2CH_2N})_2]\text{-}$ $0.5ClCH_2CH_2Cl$
M_r	1175.55
Space group	$P\bar{1}$
Crystal system	triclinic
a (Å)	19.564(3)
b (Å)	16.497(3)
c (Å)	13.243(2)
α (°)	88.93(3)
β (°)	97.88(3)
γ (°)	91.97(3)
V (Å^3)	4230.9
Z	4
$R(F_0)$	0.055
$R_w(F_0)$	0.061
Weighting scheme	$w=[\sigma^2(F_0)+0.002204(F_0)^2]^{-1}$
GOF	1.36

ml of a 1.6 M n-hexane solution) in THF (30 ml) at 0 °C. The suspension was stirred at 0 °C for 30 min and then at room temperature for 3 days. After this time, the reaction mixture was taken to dryness. The white solid obtained was washed with MeOH (3×5 ml), n-hexane (3×5 ml), Et_2O (3×5 ml) and dried under vacuum. Yield 0.151 g (65%), m.p. 282–283 °C. *Anal.* Calc. for $C_{56}H_{52}N_4Cl_2P_2O_2Pt_2$: C, 50.34; H, 3.92; N, 4.19; Cl, 5.30. Found: C, 49.90; H, 4.01; N, 4.10; Cl, 5.12%.

X-ray structural determination

The crystal data are summarized in Table 1 together with some experimental details. The atomic coordinates are reported in Table 2 and relevant bond distances and angles in Table 3. A colorless prismatic crystal (0.36×0.30×0.18 mm) was lodged in a Lindemann glass capillary and centred on a four-circle Philips PW 1100 diffractometer with graphite-monochromated (Mo Kα radiation, $\lambda = 0.71069$ Å). The orientation matrix and preliminary unit cell dimensions were determined from 25 reflections found by mounting the crystal at random and varying each of the orientation angles θ, χ and ϕ over a range of 120°, with $5 \leqslant \theta \leqslant 7°$. For the determination of precise lattice parameters, 25 strong reflections with $10 \leqslant \theta \leqslant 13°$ were considered. Integrated intensities for *hkl* reflections in the range $h = \pm 22$, $k = \pm 18$; $l = 0$ to 14 were measured and three standard reflections, −3,3,3; −2,3,2 and −1,3,1 were monitored every 180 min. There were no significant fluctuations of intensities other than those expected from Poisson statistics. The intensity data were corrected for Lorentz–polarization effects and for absorption, by following the method of North *et al.* [17]; no correction was made for extinction. The structure was solved by using three-dimensional Patterson and Fourier techniques and refined with a blocked matrix (two blocks) because of the large number of variables, with anisotropic thermal parameters assigned to all the non-hydrogen atoms. All the hydrogen atoms were introduced in calculated positions at 0.98 Å from the carbon atom with a fixed isotropic thermal parameter.

The function minimized was $\Sigma w \Delta^2$ with $\Delta = (|F_0| - |F_c|)$. The anomalous dispersion terms [18] for Pt were taken into account in the refinement. Atomic scattering factors were taken from ref. 18. Data processing and computation were carried out by using the SHELX 76 program package [19], ORTEP for drawing [20] and PARST for geometrical calculations [21].

TABLE 2. Fractional coordinates with equivalent isotropic thermal parameters (Å×10) with e.s.d.s in parentheses

Atom	x	y	z	$U_{\mathrm{iso/eq}}$[a]	pp[b]
Pt(1)	0.07744(4)	0.36287(4)	0.53043(5)	37.9(3)	
Pt(2)	0.08681(4)	0.30422(5)	0.28752(6)	43.9(3)	
Cl(2)	0.0070(2)	0.1985(2)	0.2063(3)	37(1)	
Cl(1)	0.1763(2)	0.3535(2)	0.6638(2)	22.6(8)	
Pt(3)	0.56287(4)	0.30610(4)	0.75755(6)	39.8(3)	
Pt(4)	0.53586(4)	0.34841(4)	1.00052(5)	40.5(3)	
Cl(3)	0.6795(2)	0.2998(2)	0.7118(3)	29(1)	
Cl(4)	0.4637(2)	0.2621(2)	1.0990(3)	035(1)	
P(1)	0.0125(3)	0.2861(3)	0.6233(4)	42(2)	
P(2)	0.1789(3)	0.2341(3)	0.2610(4)	45(2)	
C(1)	0.141(1)	0.397(1)	0.346(2)	49(7)	
N(2)	0.0023(9)	0.3636(9)	0.324(1)	55(7)	
C(4)	0.0021(9)	0.378(1)	0.422(2)	43(7)	
O(2)	−0.0579(7)	0.4143(7)	0.440(1)	51(5)	
O(1)	0.1864(7)	0.4379(8)	0.294(1)	60(6)	
N(1)	0.1381(8)	0.4244(8)	0.436(1)	50(6)	
C(2)	0.222(1)	0.500(1)	0.363(2)	71(10)	
C(3)	0.186(1)	0.495(1)	0.457(1)	48(7)	
C(5)	−0.103(1)	0.421(1)	0.339(2)	65(9)	
C(6)	−0.061(1)	0.385(1)	0.265(2)	55(8)	
C(7)	−0.001(1)	0.330(1)	0.742(1)	43(7)	
C(8)	−0.032(1)	0.406(1)	0.742(2)	67(9)	
C(9)	−0.043(1)	0.445(1)	0.827(2)	76(11)	
C(10)	−0.016(1)	0.410(1)	0.918(2)	69(9)	
C(11)	0.017(1)	0.339(1)	0.927(2)	77(11)	
C(12)	0.024(1)	0.301(1)	0.833(2)	63(9)	
C(13)	0.042(1)	0.186(1)	0.656(1)	51(8)	
C(14)	0.105(1)	0.159(1)	0.625(2)	63(9)	
C(15)	0.124(2)	0.080(1)	0.649(2)	82(12)	
C(16)	0.089(2)	0.030(2)	0.695(2)	98(14)	
C(17)	0.025(2)	0.053(2)	0.730(2)	96(13)	
C(18)	0.002(1)	0.133(1)	0.705(2)	73(9)	
C(19)	−0.074(1)	0.258(1)	0.558(2)	55(8)	
C(20)	−0.077(1)	0.219(1)	0.468(2)	53(8)	
C(21)	−0.140(1)	0.194(1)	0.414(2)	65(9)	
C(22)	−0.198(1)	0.208(1)	0.448(2)	72(10)	
C(23)	−0.197(1)	0.247(1)	0.542(2)	66(9)	
C(24)	−0.136(1)	0.269(1)	0.594(2)	55(9)	
C(25)	0.189(1)	0.229(1)	0.125(1)	46(7)	
C(26)	0.208(1)	0.297(1)	0.074(2)	60(8)	
C(27)	0.210(1)	0.296(2)	−0.028(2)	78(11)	
C(28)	0.196(1)	0.226(2)	−0.084(2)	72(10)	
C(29)	0.180(1)	0.157(2)	−0.031(2)	83(12)	
C(30)	0.172(1)	0.160(1)	0.073(2)	67(9)	
C(31)	0.181(1)	0.133(1)	0.309(1)	49(8)	
C(32)	0.238(2)	0.088(1)	0.299(2)	102(13)	
C(33)	0.242(2)	0.004(2)	0.334(3)	139(18)	
C(34)	0.186(3)	−0.028(2)	0.389(3)	147(21)	
C(35)	0.136(2)	0.018(2)	0.400(2)	118(16)	
C(36)	0.134(1)	0.096(1)	0.361(2)	78(10)	
C(37)	0.261(1)	0.273(1)	0.325(2)	52(8)	
C(38)	0.321(1)	0.285(1)	0.276(2)	56(8)	
C(39)	0.381(1)	0.315(2)	0.334(2)	95(13)	
C(40)	0.386(1)	0.333(2)	0.440(2)	83(12)	
C(41)	0.326(1)	0.323(1)	0.480(2)	73(10)	
C(42)	0.264(1)	0.292(1)	0.428(1)	56(9)	
P(3)	0.6299(3)	0.3421(3)	1.1160(4)	53(2)	
P(4)	0.5349(3)	0.1786(3)	0.7080(4)	45(2)	
N(3)	0.5886(8)	0.4160(9)	0.822(1)	43(5)	
N(4)	0.4571(8)	0.3463(9)	0.880(1)	45(6)	
O(3)	0.6030(7)	0.4993(7)	0.9560(9)	53(5)	

(*continued*)

TABLE 2 (*continued*)

Atom	x	y	z	$U_{iso/eq}$ [a]	pp [b]
O(4)	0.4150(7)	0.3287(8)	0.717(1)	55(5)	
C(1)A	0.5793(9)	0.4270(9)	0.916(1)	40(6)	
C(2)A	0.626(1)	0.489(1)	0.785(2)	66(10)	
C(3)A	0.636(1)	0.543(1)	0.875(2)	80(11)	
C(4)A	0.470(1)	0.327(1)	0.791(1)	48(8)	
C(5)A	0.356(1)	0.351(1)	0.764(2)	72(10)	
C(6)A	0.3818(9)	0.361(1)	0.873(2)	73(10)	
C(7)A	0.621(1)	0.379(1)	1.242(2)	57(8)	
C(8)A	0.568(1)	0.439(1)	1.246(2)	66(10)	
C(9)A	0.561(1)	0.472(2)	1.339(2)	78(11)	
C(10)A	0.600(2)	0.446(2)	1.427(2)	88(11)	
C(11)A	0.648(2)	0.381(2)	1.423(2)	108(15)	
C(12)A	0.659(1)	0.358(1)	1.330(2)	87(11)	
C(13)A	0.706(1)	0.398(1)	1.083(2)	60(8)	
C(14)A	0.742(1)	0.456(1)	1.149(2)	62(9)	
C(15)A	0.800(2)	0.497(1)	1.113(3)	96(14)	
C(16)A	0.822(1)	0.480(2)	1.021(3)	105(15)	
C(17)A	0.787(1)	0.421(2)	0.960(2)	89(11)	
C(18)A	0.730(1)	0.378(1)	0.993(2)	77(11)	
C(19)A	0.662(1)	0.240(1)	1.135(2)	72(9)	
C(20)A	0.733(2)	0.224(2)	1.169(2)	159(18)	
C(21)A	0.760(2)	0.151(2)	1.179(3)	174(20)	
C(22)A	0.708(4)	0.082(3)	1.164(3)	231(34)	
C(23)A	0.640(3)	0.090(3)	1.129(4)	193(28)	
C(24)A	0.618(2)	0.171(2)	1.119(2)	115(16)	
C(25)A	0.444(1)	0.149(1)	0.715(2)	57(9)	
C(26)A	0.424(1)	0.148(1)	0.811(2)	74(10)	
C(27)A	0.354(2)	0.134(2)	0.826(2)	100(13)	
C(28)A	0.306(2)	0.123(2)	0.724(4)	158(23)	
C(29)A	0.327(2)	0.127(2)	0.633(3)	112(16)	
C(30)A	0.394(1)	0.140(1)	0.629(2)	71(10)	
C(31)A	0.580(1)	0.098(1)	0.786(2)	59(9)	
C(32)A	0.644(1)	0.113(2)	0.835(2)	77(9)	
C(33)A	0.673(2)	0.043(2)	0.891(2)	116(16)	
C(34)A	0.649(2)	−0.025(2)	0.893(2)	94(12)	
C(35)A	0.584(2)	−0.038(2)	0.840(3)	120(16)	
C(36)A	0.550(2)	0.021(1)	0.790(2)	102(14)	
C(37)A	0.548(1)	0.158(1)	0.577(1)	54(7)	
C(38)A	0.540(2)	0.215(2)	0.508(2)	110(15)	
C(39)A	0.546(2)	0.200(2)	0.402(2)	101(14)	
C(40)A	0.568(2)	0.124(2)	0.385(3)	130(16)	
C(41)A	0.576(3)	0.070(2)	0.446(3)	184(23)	
C(42)A	0.571(2)	0.083(2)	0.555(3)	162(21)	
Cl(5)	0.8365(9)	0.207(1)	0.861(1)	114(5)*	0.5
Cl(6)	0.899(2)	0.041(2)	0.968(2)	218(12)*	0.5
C(43)	0.885(3)	0.187(4)	0.981(5)	102(18)*	0.5
C(44)	0.934(5)	0.134(5)	0.988(6)	154(30)*	0.5

[a] U_{eq} is defined as one third of the trace of the orthogonalized U_{ij} tensor; U_{iso} are starred. [b] pp = parameters population.

Results and discussion

Synthesis of carbene complexes

One or both the RNC ligands in the complexes cis-$Cl_2(PPh_3)Pt(CNBu^t)$ and cis-$Cl_2Pt(CNC_6H_4$-p-$OMe)_2$ are converted to the cyclic diaminocarbenes cis-$Cl_2(PPh_3)Pt[\overline{CN(Bu^t)CH_2CH_2NH}]$ (**1**) and cis-$Cl_2Pt[\overline{CN(C_6H_4\text{-}p\text{-}OMe)CH_2CH_2NH}]_2$ (**2**), respectively, according to Scheme 1.

Similar reactions have been reported for the conversion of isocyanide and carbonyl ligands in Pt(II) complexes to cyclic aminocarbenes [1a, 6, 22]. It is observed (Scheme 1) that for the sterically hindered Bu^t isocyanide the reaction proceeds to the final complex **1** only in the presence of aziridine/$ClCH_2CH_2NH_3^+Cl^-$, while both the CNC_6H_4-p-OMe ligands react with aziridine alone to give **2**.

There is no *cis–trans* isomerization during the reactions as evidenced by the presence of two Pt–Cl absorptions in the IR spectrum, indicating a *cis* stereogeometry for **1** and **2** (Table 4) [16]. On the

TABLE 3. Selected bond angles (°) and distances (Å) with e.s.d.s in parentheses

Dimer I		Dimer II	
Bond angles			
C(4)–Pt(1)–N(1)	85.9(7)	N(3)–Pt(3)–C(4)A	84.4(7)
P(1)–Pt(1)–N(1)	174.5(4)	P(4)–Pt(3)–C(4)A	93.8(6)
P(1)–Pt(1)–C(4)	92.9(5)	P(4)–Pt(3)–N(3)	172.2(4)
Cl(1)–Pt(1)–N(1)	90.6(5)	Cl(3)–Pt(3)–C(4)A	172.3(6)
Cl(1)–Pt(1)–C(4)	175.8(6)	Cl(3)–Pt(3)–N(3)	89.4(5)
Cl(1)–Pt(1)–P(1)	90.8(2)	Cl(3)–Pt(3)–P(4)	93.0(2)
Pt(2)–Pt(1)–N(1)	57.2(5)	Pt(4)–Pt(3)–C(4)A	58.5(6)
Pt(2)–Pt(1)–C(4)	58.4(6)	Pt(4)–Pt(3)–N(3)	57.6(4)
Pt(2)–Pt(1)–P(1)	117.7(1)	Pt(4)–Pt(3)–P(4)	115.1(1)
Pt(2)–Pt(1)–Cl(1)	121.3(1)	Pt(4)–Pt(3)–Cl(3)	121.3(1)
Pt(1)–Pt(2)–N(2)	58.6(5)	Pt(3)–Pt(4)–C(1)A	57.8(6)
Pt(1)–Pt(2)–C(1)	59.0(6)	Pt(3)–Pt(4)–N(4)	57.8(4)
Pt(1)–Pt(2)–P(2)	117.4(1)	Pt(3)–Pt(4)–P(3)	114.4(2)
Pt(1)–Pt(2)–Cl(2)	120.7(1)	Pt(3)–Pt(4)–Cl(4)	123.3(1)
C(1)–Pt(2)–N(2)	85.7(7)	N(4)–Pt(4)–C(1)A	84.1(7)
P(2)–Pt(2)–N(2)	175.0(5)	P(3)–Pt(4)–C(1)A	93.0(6)
P(2)–Pt(2)–C(1)	94.5(6)	P(3)–Pt(4)–N(4)	171.9(4)
Cl(2)–Pt(2)–N(2)	88.5(5)	Cl(4)–Pt(4)–C(1)A	170.5(5)
Cl(2)–Pt(2)–C(1)	173.1(6)	Cl(4)–Pt(4)–N(4)	89.1(4)
Cl(2)–Pt(2)–P(2)	91.5(2)	Cl(4)–Pt(4)–P(3)	94.7(2)
Pt(1)–P(1)–C(19)	114.8(7)	Pt(4)–P(3)–C(19)A	113.1(8)
Pt(1)–P(1)–C(13)	116.2(7)	Pt(4)–P(3)–C(13)A	115.6(7)
Pt(1)–P(1)–C(7)	114.3(7)	Pt(4)–P(3)–C(7)A	115.5(8)
Pt(2)–P(2)–C(37)	115.1(7)	Pt(3)–P(4)–C(37)A	114.3(7)
Pt(2)–P(2)–C(31)	116.0(7)	Pt(3)–P(4)–C(31)A	115.9(7)
Pt(2)–P(2)–C(25)	112.5(6)	Pt(3)–P(4)–C(25)A	113.4(7)
Pt(2)–C(1)–N(1)	124(1)	Pt(3)–N(3)–C(2)A	132(1)
Pt(2)–C(1)–O(1)	121(1)	Pt(3)–N(3)–C(1)A	119(1)
Pt(2)–N(2)–C(6)	132(1)	Pt(4)–N(4)–C(6)A	132(1)
Pt(2)–N(2)–C(4)	116(1)	Pt(4)–N(4)–C(4)A	120(1)
Pt(1)–C(4)–N(2)	127(1)	C(1)A–N(3)–C(2)A	109(1)
Pt(1)–C(4)–O(2)	121(1)	C(1)A–O(3)–C(3)A	106(1)
Pt(1)–N(1)–C(1)	120(1)	C(4)A–O(4)–C(5)A	107(1)
Pt(1)–N(1)–C(3)	130(1)	C(4)A–N(4)–C(6)A	108(1)
C(4)–N(2)–C(6)	111(1)	N(3)–C(1)A–O(3)	116(1)
C(1)–O(1)–C(2)	106(1)	Pt(4)–C(1)A–O(3)	119(1)
C(1)–N(1)–C(3)	110(1)	Pt(4)–C(1)A–N(3)	125(1)
C(4)–O(2)–C(5)	108(1)	N(3)–C(2)A–C(3)A	104(1)
O(1)–C(1)–N(1)	115(1)	O(3)–C(3)A–C(2)A	106(1)
N(2)–C(4)–O(2)	112(1)	N(4)–C(4)A–O(4)	115(1)
O(1)–C(2)–C(3)	106(1)	Pt(3)–C(4)A–O(4)	121(1)
N(1)–C(3)–C(2)	102(1)	Pt(3)–C(4)A–N(4)	124(1)
O(2)–C(5)–C(6)	104(1)	O(4)–C(5)A–C(6)A	106(1)
N(2)–C(6)–C(5)	106(1)	N(4)–C(6)A–C(5)A	104(1)

(*continued*)

TABLE 3 (*continued*)

Dimer I		Dimer II	
Bond distances			
Pt(1)–Pt(2)	3.407(1)	Pt(3)–Pt(4)	3.420(1)
Pt(1)–Cl(1)	2.441(3)	Pt(3)–Cl(3)	2.447(4)
Pt(1)–P(1)	2.233(5)	Pt(3)–P(4)	2.243(5)
Pt(2)–Cl(2)	2.462(4)	Pt(4)–Cl(4)	2.452(4)
Pt(2)–P(2)	2.245(6)	Pt(4)–P(3)	2.229(6)
Pt(1)–C(4)	1.93(2)	Pt(4)–N(4)	2.06(1)
Pt(1)–N(1)	2.07(2)	Pt(3)–N(3)	2.04(1)
Pt(2)–C(1)	1.96(2)	Pt(3)–C(4)A	1.98(2)
Pt(2)–N(2)	2.07(2)	Pt(4)–C(1)A	1.95(2)
P(1)–C(7)	1.80(2)	P(3)–C(7)A	1.83(2)
P(1)–C(13)	1.80(2)	P(3)–C(13)A	1.82(2)
P(1)–C(19)	1.85(2)	P(3)–C(19)A	1.83(2)
P(2)–C(25)	1.84(2)	P(4)–C(25)A	1.85(2)
P(2)–C(31)	1.77(2)	P(4)–C(31)A	1.83(2)
P(2)–C(37)	1.81(2)	P(4)–C(37)A	1.82(2)
C(1)–O(1)	1.35(3)	N(3)–C(1)A	1.29(2)
C(1)–N(1)	1.28(3)	N(3)–C(2)A	1.50(3)
N(2)–C(4)	1.33(3)	N(4)–C(4)A	1.29(3)
N(2)–C(6)	1.43(2)	N(4)–C(6)A	1.49(2)
C(4)–O(2)	1.38(2)	O(3)–C(1)A	1.36(2)
O(2)–C(5)	1.50(2)	O(3)–C(3)A	1.49(3)
O(1)–C(2)	1.48(2)	O(4)–C(4)A	1.34(2)
N(1)–C(3)	1.48(2)	O(4)–C(5)A	1.45(3)
C(2)–C(3)	1.51(3)	C(2)A–C(3)A	1.49(3)
C(5)–C(6)	1.50(3)	C(5)A–C(6)A	1.48(3)

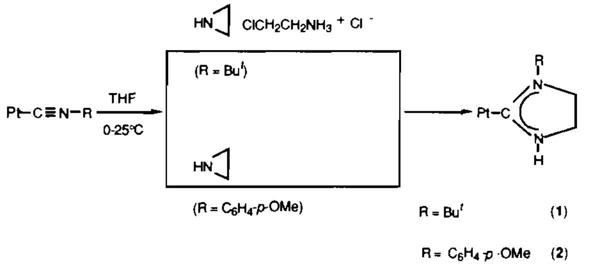

Scheme 1.

other hand, the ^{1}H NMR spectrum of **1** in CD_2Cl_2 shows the presence of two signals (3:1 ratio) due to the Bu^t group (see Table 4), which are likely to arise from mutual different arrangements of the highly hindered Bu^t group of the carbene ligands with respect to the phosphine. In the ^{31}P NMR spectrum only the most abundant compound is observed probably due to the low solubility of compound **1**. For **2**, four isomers are observed in the ^{1}H NMR spectrum, which are likely to arise from mutual different arrangements of the two carbene ligands: four singlets of the OCH_3 group are observed in the ratio 1:1:0.1:0.1 the signals at δ 3.87 and 3.77 being the most intense. Four signals of the NH proton are also observed in the range δ 8.99–10.00.

The bis-aminooxycarbene compound *cis*-$Cl_2Pt[\overline{CN(C_6H_4\text{-}p\text{-}OMe)CH_2CH_2O}]_2$ (**3**) was obtained by reaction of 2.2 equiv. of $^-OCH_2CH_2Cl$ (from $HOCH_2CH_2Cl$ and n-BuLi) with the corresponding bis-isocyanide complex, by a procedure similar to that we have reported previously [1b]. The presence in the IR spectrum of two absorptions at 318 and 296 cm^{-1} indicates for compound **3** a *cis* stereogeometry. ^{1}H NMR data (Table 4) indicate that **3** is present in only one isomeric form.

Reactions with n-BuLi

It has been reported that the aminooxy- [2] and diaminocarbene [1a] ligands are deprotonated by bases to give imino derivatives whose nitrogen reacts with electrophiles to regenerate carbene complexes. We also described recently that the neutral aminooxy carbene compound *cis*-$Cl_2(PPh_3)Pt[\overline{COCH_2CH_2NH}]$ [22] reacts with n-BuLi leading to the formation of the dimer $\{(PPh_3)ClPt[\mu\text{-}\overline{COCH_2CH_2N}\text{-}C,N]\}_2$ (**7**), whose X-ray structure is discussed below.

Analogous reactions occur by reacting neutral diaminocarbene compounds *cis*-$Br_2(PPh_3)Pd[\overline{CN(Me)CH_2CH_2NH}]$ [1a], *cis*-$Cl_2(PPh_3)Pd[\overline{CN(C_6H_4\text{-}p\text{-}OMe)CH_2CH_2NH}]$ [16] and *cis*-$Cl_2(PPh_3)Pt[\overline{CN(C_6H_4\text{-}p\text{-}OMe)CH_2CH_2NH}]$ [16] with n-BuLi, the dimeric compounds **4**–**6** being formed, respectively, according to eqn. (1). As observed for similar reactions with neutral aminocarbenes [22], reactions (1) also do not yield any N–R derivatives when carried out in the presence of an excess of R–X electrophiles ($R = CH_2CH{=}CH_2$, $CH_2{-}C{\equiv}CH$). However, this behavior contrasts markedly with that shown by cationic aminocarbene complexes [1a, 22]. Compounds **4**–**6** were characterized by elemental analyses and spectroscopic data (Table 4) and, for **4** and **5**, also by their FAB mass spectra. The ^{31}P NMR spectra of **4**–**6** show only one resonance indicating the presence in solution of one isomer probably being that having the PPh_3 ligand *cis* to the carbene group as found for $\{(PPh_3)ClPt[\mu\text{-}\overline{COCH_2CH_2N}\text{-}C,N]\}_2$ (**7**) (see below). Furthermore, the Pt complex **6** shows $^1J(P\text{-}Pt) = 3590$ Hz which agrees with a *trans*-P–M–N arrangement [22]. The ^{1}H NMR spectra of **4**–**6** (Table 4) show four multiplets, one for each proton, for the $-NCH_2CH_2N-$ moiety of the carbene ligand as observed for similar systems [16].

Description of the structure of $\{(PPh_3)ClPt[\mu\text{-}\overline{COCH_2CH_2N}\text{-}C,N]\}_2$ *(7)*

The molecular structure of $\{(PPh_3)ClPt[\mu\text{-}\overline{COCH_2CH_2N}\text{-}C,N]\}_2$ (**7**) is shown in Fig. 1 together with the atom labelling. The crystal contains two crystallographically independent dimer units $\{(PPh_3)ClPt[\mu\text{-}\overline{COCH_2CH_2N}\text{-}C,N]\}_2$ and a disordered dichloroethane molecule. Each dimer is formed by two bridging L ($L = \overline{COCH_2CH_2N}$) which are

TABLE 4. Selected IR, ^{1}H NMR and ^{31}P NMR data of carbene complexes of Pd(II) and Pt(II)

Compound	IR^a			^{1}HNMR^b			^{31}P NMR^c	
	ν(C=N)	ν(NH)	ν(MCl)	δ(NCH$_2$)	δ(NH)	δ(other)	δ(P)	^1J(P–Pt)
1	1508 s	3295 s	306 m	3.48 m	6.64 br	1.63 s^d	7.79 s	4105
			281 w	3.06 m		1.54 s^d		
2	1511 s	3141 m	310 br	3.88–3.78 m	9.62	3.87 s^e		
					8.99	3.77 s^e		
					10.00	3.85 s^e		
					9.93	3.80 s^e		
3^f	1513 s		318 w	4.04 t		3.81 s^e		
			294 w	$^3J_{(HH)}$9.8		4.52 t^g		
4	1509 s			3.88 m		2.58 s^h	26.10 s	
				3.38 m				
				2.66 m				
				2.14 m				
5	1503 s		273 m	4.10 m		3.79 s^e	23.0 s	
				3.80 m				
				3.00 m				
				2.82 m				
6	1501 s		294 m	4.24 m		3.79 s^e	6.04 s	3590
				3.65 m				
				3.16 m				
				2.99 m				

[a] Spectra recorded as Nujol mulls; ν in cm^{-1}. Abbreviations: s = strong; m = medium; w = weak; br = broad. [b] ^{1}H NMR spectra recorded in CD$_2$Cl$_2$ unless otherwise stated. Proton chemical shifts are referenced to Me$_4$Si by taking the chemical shift of dichloromethane-d$_2$ as +5.32 ppm; J in Hz; s = singlet; t = triplet; m = multiplet; br = broad. [c] Spectra recorded in CD$_2$Cl$_2$ unless otherwise stated, with H$_3$PO$_4$ as external reference; J in Hz; s = singlet. [d] Bu^t. [e] OCH$_3$. [f] ^{1}H NMR and ^{31}P NMR spectra recorded in DMSO-d$_6$. [g] OCH$_2$. [h] Me.

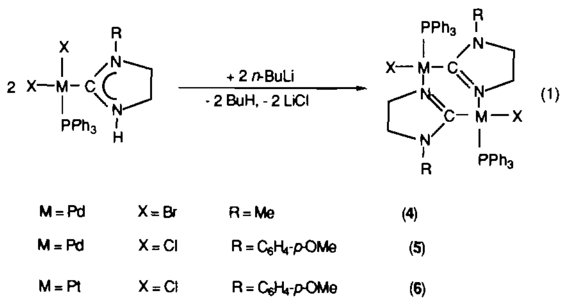

Scheme 2.

coordinated to one platinum on one side via a Pt–N bond and to the second platinum via a Pt–C bond. The coordination geometry around each platinum atom is an irregular square with deviations in the tetrahedral direction of the bonded atoms (from −0.15(2) to 0.16(2) Å for the Pt(1)...Pt(2) dimer and from −0.24(2) to 0.25(2) Å for the Pt(3)...Pt(4) dimer).

The two Pt coordination planes in each dimer are roughly orthogonally oriented: 90.3(2) and 90.0(2)° are the respective values of the angles between the planes containing Pt(1) and Pt(2) and, in the second dimer, Pt(3) and Pt(4). The hexaatomic ring formed by two Pt atoms and the nitrogen and carbon atoms of the L bridging ligand has in both dimers a boat conformation (the apices are in both cases the metal ions) and the two L ligands are oriented in opposite directions with respect to the boat apices in order to minimize molecular strains. The dihedral angles between the two L planes are 69.7(7) and 73.1(8)° for dimer I and dimer II, respectively. The two dimers differ slightly in the orientation of the L ligands as well as for that of the phosphine phenyls while analogous bond distances and angles are comparable in both.

The Cl–Pt–C and P–Pt–N systems show slight bending in all four coordination 'planes' with angular values close on average to 175(1)° for dimer I and to 172(1)° for dimer II. This could be related to steric interaction between the bulky triphenylphosphine ligands and the bridging carbenoid systems.

The Pt–P distances (average 2.237(5) Å) are comparable to the value of 2.235(2) Å found in *cis*-Br$_2$(PPh$_3$)Pt[$\overline{\text{CN(C}_6\text{H}_4\text{-}p\text{-Me)CH}_2\text{CH}_2\text{N}}$H] [1a] and 2.220(2) Å found in *cis*-Cl$_2$(PPh$_3$)Pt[CHN(Me)$_2$] [23] where the triphenylphosphine ligand is *trans* to a bromine or chlorine, while in the present determination is *trans* to nitrogen. This could suggest that the Pt–P distances are mainly influenced by steric factors (rather than by electronic factors) which

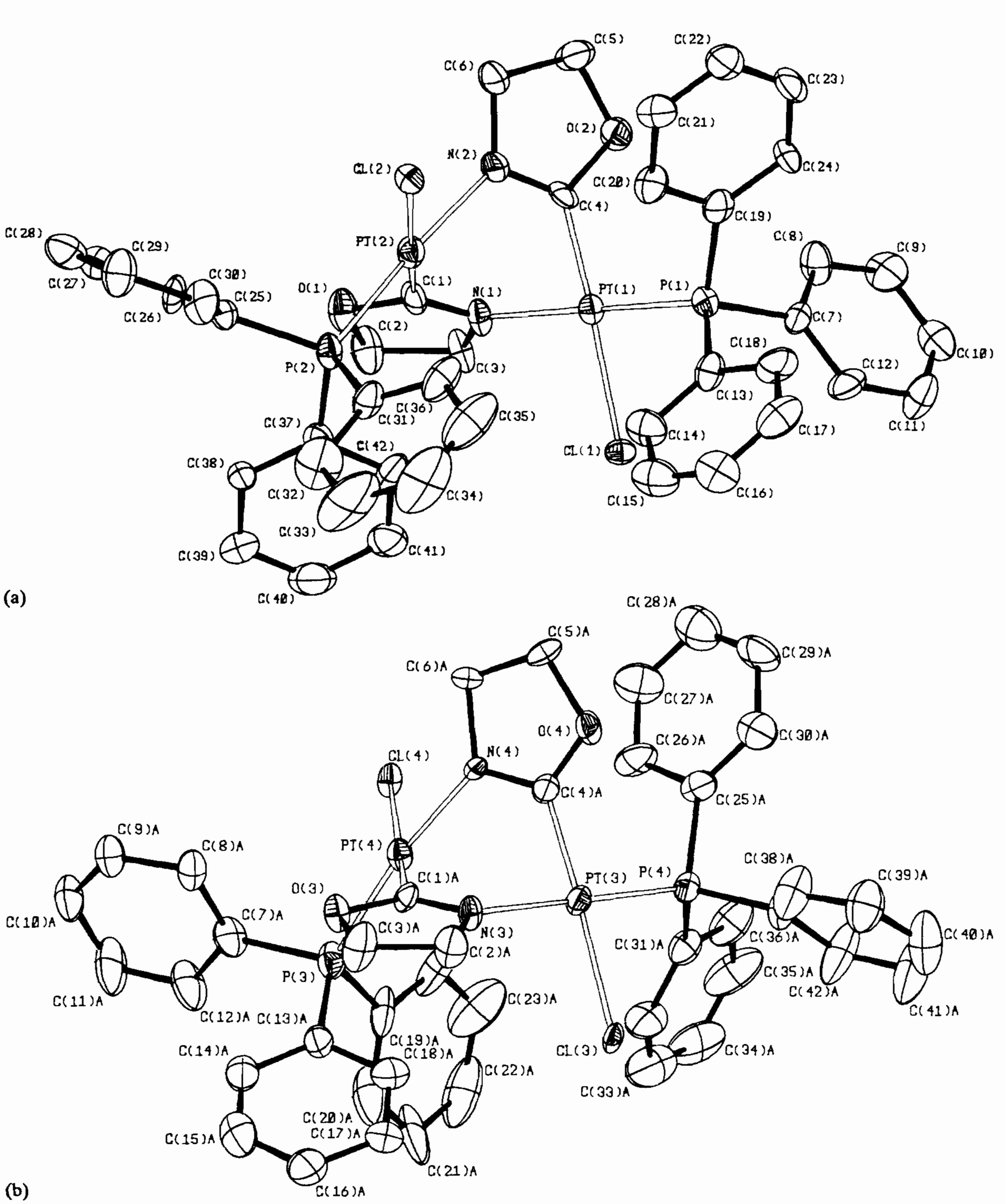

Fig. 1. Molecular structure of $\{(PPh_3)ClPt[\mu\text{-}COCH_2CH_2N\text{-}C,N]\}_2$: (a) dimer I; (b) dimer II.

hinder a closer coordination of a bulky ligand. The Pt–Cl bond lengths (2.450(4) Å on average) exceed the values normally found in Pt(II) carbene complexes as *cis*-$Cl_2(Et_3P)Pt[C(OEt)NHPh]$ (Pt–Cl (*trans* to carbene) = 2.361(5) Å) [23] but are comparable to the values of 2.431(3) Å found in *trans*-$(PPh_3)_2Pt(Me)Cl$ [24] where a strong σ-donor methyl group is *trans* to chloride. This lengthening in the Pt–Cl distances agrees with the observation of the good σ-donor but poor π-acceptor properties of carbenes in Pt(II) systems [25]. On the other hand the short values for Pt–C distances (1.95(2) Å on average) should indicate the strong σ-interaction and weak *trans* influence of chlorine. In any case, these values are in the range (1.82–2.01 Å) of the values found when chlorine is *trans* to the carbene ligand [26]. The Pt–N bond distances (2.06(2) Å on average) are between the value of 2.011(3)Å found in *cis*-$Cl_2Pt[\overline{NC(Ph)OCH_2CH_2}]_2$ [27a] and the value of 2.10(1) Å (N *trans* to C) found in (dad)$\overline{PtOOCMe_2C(=CH_2)C(=CMe_2)CH_2}$ (dad = diazadiene) [27b] but is shorter with respect to the value of 2.156(5) Å for a Pt–N *trans* to a PPh_3 ligand in $[(\eta^2\text{-Hcyclen-P})Pt(Cl)(PPh_3)]BF_4$ [28].

The cyclic carbene ligands are planar as observed in *trans*-$\{(PPh_3)_2Pt[\overline{CN(C_6H_4\text{-}p\text{-}Me)CH_2CH_2O}Br\}^+$ [1b], where the Pt–C distance of 1.98(1) Å is comparable to the value of 1.95(2) Å found in the present determination. The high standard deviations do not allow a detailed discussion of bond distances within the bridging ligand L. However, the values found are comparable with those reported in aminooxycarbene compounds [1] and are indicative of substantial multiple bond character for the C–N bond, with a significant π-bonding interaction which involves not only the nitrogen and the carbene carbon but also the oxygen atom.

Electrochemical studies

By cyclic voltammetry (CV), the monocarbene complex (**1**) or the analogous *cis*-$Cl_2PdL[\overline{CN(Bu^t)CH_2CH_2NH}]$ (L = PPh_3 or $CNBu^t$) (Table 5), in 0.2 mol dm^{-3} $[Bu_4N][BF_4]$/NCMe and at a Pt electrode, undergo an irreversible anodic process at an oxidation potential (E_p^{ox} = *c.* 1.8–1.9 V versus SCE) which is only marginally affected by the metal (Pd or Pt) or the ligand L. By controlled potential electrolysis (CPE), this wave involves *c.* two electrons (1.9–1.7 e^-) with evolution of *c.* $2H^+$. The proton emission has been measured by acid–base titration [15] of each of the electrochemically oxidized complex solutions and corrected for background effects by considering also the titration of the corresponding blank solution of the electrolyte following its electrolysis under conditions which were identical to those applied to the complex solution; the corrected values were obtained by subtracting the background values from those directly derived from the titration of the electrolyzed solution of the complex.

The cyclic voltammograms of the dicarbenes **2** and **3** are more complex, mainly for the former compound, with two secondary amino groups, which presents four anodic waves (the central ones, at E_p^{ox} = *c.* 1.4 V, overlap extensively and are denoted under the common heading II in Table 5). The first wave (I) for these species occurs at lower potentials (E_p^{ox} = 1.20 or 1.65 V, respectively) than those observed for the above-mentioned monocarbene complexes, but proton evolution is also detected. In fact, upon CPE at this wave, liberation of *c.* one proton in a single-electron process or of *c.* two protons in a two-electron transfer is observed for complex **2** or **3**, respectively, whereas their second anodic waves (at E_p^{ox} = 1.35 and 1.46 V for the former or 1.86 V for the latter) involve multielectron (*c.* 4 electrons, by exhaustive CPE) and multiproton loss processes (*c.* $4H^+$ as measured by acid–base titration).

In these complexes the aminocarbene ligands are the only possible proton source and, therefore, the oxidation processes involve anodically-induced deprotonation of such ligands, conceivably resulting from N–H and/or C–H bond cleavage, the former at a secondary amino group and the latter at a methylene group [29] activated by an adjacent amino or oxy moiety. Such processes can lead to imine-type species, as suggested by the known [30] stepwise oxidative dehydrogenation of chelated amines. However, they appear to have been observed in this study for the first time at amino- or aminooxy-carbene ligands, although we have failed to isolate pure species from the electrolyzed solutions.

It is also noteworthy that the oxycarbene **3** is much harder to oxidize than the analogous carbene complex **2** with a secondary amino group (E_p^{ox} = 1.65 and 1.20 V, respectively), thus following the known [29] higher resistance of ethers, compared to amines, towards oxidation. A related trend is observed at the dinuclear dicarbene complexes discussed below and these observations suggest that the first anodic process may be ligand centred.

However, this order for the values of the oxidation potential also agrees with that predicted for metal-centred processes (although possibly a less pronounced difference in those values should be expected – see below) since an oxycarbene should behave as a weaker electron-donor than an aminocarbene ligand, as known [7] to occur in $[Cr(CO)_5(carbene)]$ (the oxycarbene species being oxidized at *c.* 0.12–0.16 V more anodic potentials than the aminocarbene complexes).

Moreover, the electrochemical oxidation to Pt(IV) of some neutral *cis*- or *trans*-dichloro complexes of Pt(II) of the type $[PtCl_2(PR_3)_2]$ has been reported [31] to occur in the *c.* 1.8–2.0 V range, i.e., similar to that observed in the monocarbene complexes of this study, but well above that presented by either the mononuclear (see above) or the dinuclear (see below) diaminocarbene species (0.8–1.2 V) which, however, is close to that quoted [32] (1.0–1.3 V) for the oxidation potential of free aliphatic secondary amines in acetonitrile; these observations suggest that the oxidation process for the monocarbene

TABLE 5. Summary of electrochemical[a] and acid–base titration data for some carbene complexes of Pd(II) or Pt(II)

Complexes	E_p^{ox} (V)[b]			CPE	
	I	II	III	n(e$^-$)	n(H$^+$)[c]
Monocarbenes					
cis-$\mathrm{Cl_2Pt(PPh_3)[\overline{CN(Bu^t)CH_2CH_2N}H]}$ (**1**)	1.92			1.9	2.0
cis-$\mathrm{Cl_2Pd(PPh_3)[\overline{CN(Bu^t)CH_2CH_2N}H]}$	1.86			1.9	1.9
cis-$\mathrm{Cl_2Pd(CNBu^t)[\overline{CN(Bu^t)CH_2CH_2N}H]}$	1.78			1.7	1.9
Dicarbenes					
cis-$\mathrm{Cl_2Pt[\overline{CN(C_6H_4\text{-}\mathit{p}\text{-}OMe)CH_2CH_2NH}\}_2}$ (**2**)	1.20	1.35, 1.46	2.0	0.9(I) 3.9(II)	0.8(I) 3.6(II)
cis-$\mathrm{Cl_2Pt[\overline{CN(C_6H_4\text{-}\mathit{p}\text{-}OMe)CH_2CH_2O}]_2}$ (**3**)	1.65	1.86		2.3(I) 4.0(II)	2.0(I) 4(II)
Dinuclear dicarbenes					
$\mathrm{\{(PPh_3)ClPd[\mu\text{-}\overline{CN(C_6H_4\text{-}\mathit{p}\text{-}OMe)CH_2CH_2N}\text{-}\mathit{C,N}]\}_2}$ (**5**)	0.96, 1.10	1.58		1.8(I) 4.1(II)	1.8(I) 3.4(II)
$\mathrm{\{(PPh_3)ClPd[\mu\text{-}\overline{CN(Me)CH_2CH_2N}\text{-}\mathit{C,N}]\}_2}$	0.80, 1.12	1.44	1.80	1.9(I)	1.7(I)
$\mathrm{\{(PPh_3)ClPt[\mu\text{-}\overline{CN(C_6H_4\text{-}\mathit{p}\text{-}OMe)CH_2CH_2N}\text{-}\mathit{C,N}]\}_2}$ (**6**)	0.98, 1.13	1.60	1.88	2.0(I) 4.0(II)	2.0(I) 3.4(II)
$\mathrm{\{(PPh_3)ClPt[\mu\text{-}\overline{COCH_2CH_2N}\text{-}\mathit{C,N}]\}_2}$ (**7**)	1.67[d]			0.93[e]	1.1

[a] Overlapping waves at close potentials are indicated under a common heading (for waves I or II). Studies performed at a Pt wire (CV) or gauze (CPE) electrode, in NCMe (unless stated otherwise)/0.2 mol dm^{-3} $\mathrm{[Bu_4N][BF_4]}$. [b] Values in V versus SCE, measured by CV at 100 mV s^{-1}, by using as internal reference the couple $\mathrm{[Fe(\eta^5\text{-}C_5H_5)_2]^{0/+}}$ ($E_{1/2}^{ox}=0.42$ or 0.54(5) V vs. SCE, in NCMe or $\mathrm{CH_2Cl_2}$, respectively). [c] Values measured by acid–base titration of the electrolyzed solution and corrected for background effects (see text). [d] In $\mathrm{CH_2Cl_2}$ due to insufficient solubility in NCMe. Value close to the limit of the accessible range of potential. [e] In NCMe/$\mathrm{CH_2Cl_2}$ (4:1 volume ratio).

complexes can be initiated at the metal, whereas those for the dicarbenes and dinuclear dicarbenes can be centred at the amino groups of the carbene ligands. A MO theoretical study would probably help to clarify this point.

Nevertheless, either the anodic processes are initiated at the metal or at the carbene ligand, the expected resulting promotion of acidity of the amino or methylene groups agrees with the observed anodically-induced ligand deprotonation.

The dinuclear diaminocarbene complex (**5**) its methylamino analogue and **6** display an anodic behaviour similar to that described for the mononuclear dicarbene species **2** and **3**. Upon CV, under the above-mentioned experimental conditions, they undergo a sequence of irreversible anodic waves (three or four) with E_p^{ox} in the 0.8–1.9 V (versus SCE) range. The first two waves, at $E_p^{ox}=0.80$–1.13 V, overlap extensively and are indicated under a common heading (I) in Table 5 (Fig. 2); upon lowering the temperature, they appear to gain a modest degree of reversibility. By CPE, they involve an overall transfer of *c.* 2 electrons, whereas the following wave (II), at $E_p^{ox}\approx 1.4$–1.6 V, corresponds to a four-electron process, in every case with a concomitant liberation of a similar number of protons (as measured by acid–base titrations — see above).

As observed for the monocarbene complexes, the metal (Pd or Pt) only hardly affects the oxidation potential (the Pd complexes appear to be oxidized at very slightly less anodic potentials). However, this potential is clearly dependent on the composition of the carbene ligand, and the oxidation of complex **5**, with an arylamino group, occurs at a more anodic potential ($E_p^{ox}=0.96$ V) than that (0.80 V) of the analogous complex with a methylamino group. Moreover, a dramatic variation of E_p^{ox} results from the replacement of an amino by an oxy group at the carbene ligand, and the alkoxycarbene complex **7** presents the first wave at a much higher potential (1.67 V) than those observed for the other dinuclear dicarbenes (which do not exceed *c.* 1.1 V). This behaviour suggests again (see above) the occurrence of a ligand based oxidation process.

The detection of other possible anodic waves at higher potentials for complex **7** was precluded by the close potential limit imposed by the discharge of the solvent which, in this case, was $\mathrm{CH_2Cl_2}$ due to the insufficient solubility of the compound in NCMe. That anodic wave involves, by CPE, a single-electron and a single-proton loss process.

Another example of an electrochemically induced deprotonation of a platinum(II) complex has been recently reported [15] for *trans*-$\mathrm{[PtHCl(PEt_3)_2]}$, but

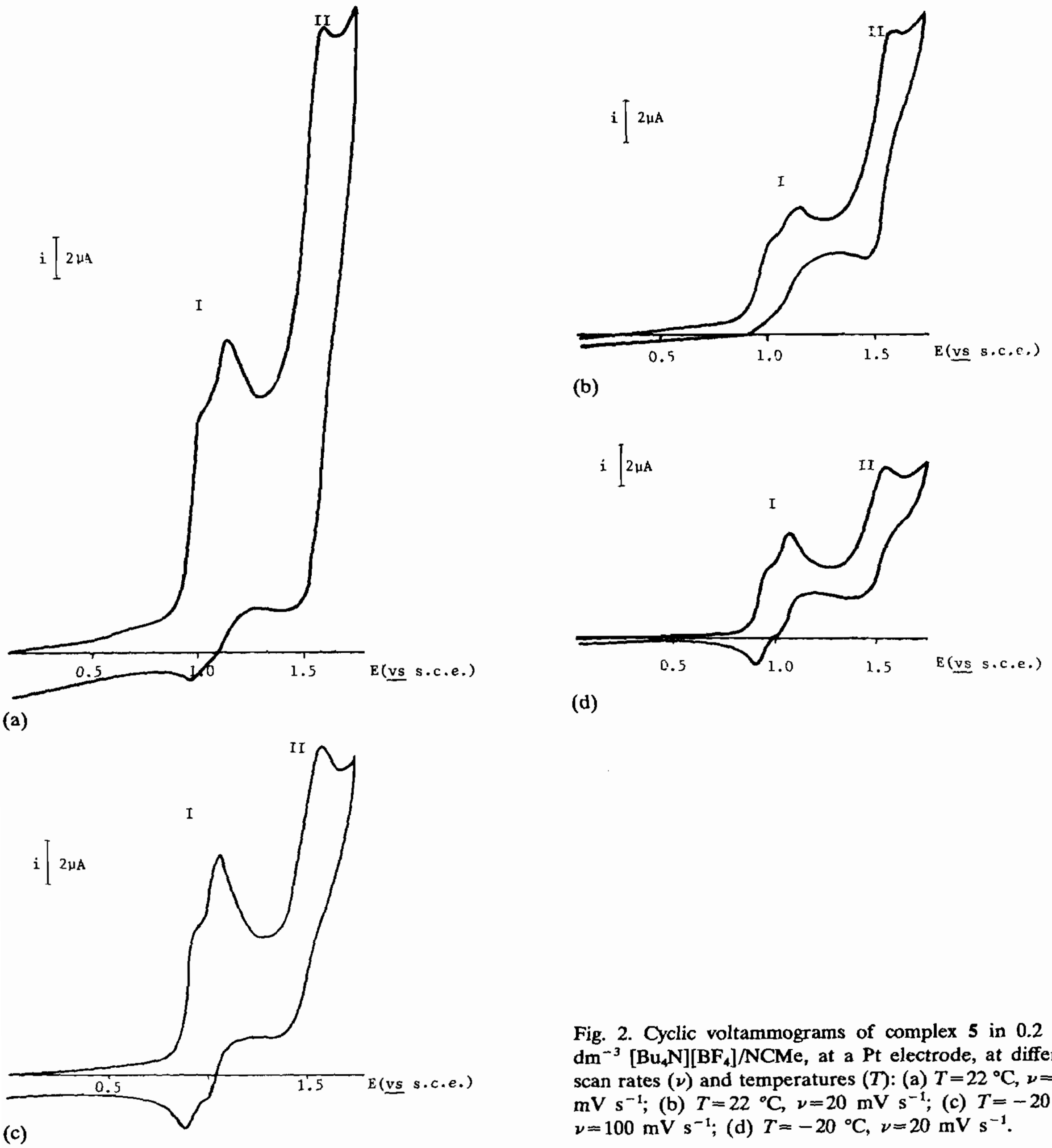

Fig. 2. Cyclic voltammograms of complex 5 in 0.2 mol dm^{-3} [Bu$_4$N][BF$_4$]/NCMe, at a Pt electrode, at different scan rates (ν) and temperatures (T): (a) $T=22$ °C, $\nu=100$ mV s^{-1}; (b) $T=22$ °C, $\nu=20$ mV s^{-1}; (c) $T=-20$ °C, $\nu=100$ mV s^{-1}; (d) $T=-20$ °C, $\nu=20$ mV s^{-1}.

it involves a metal–hydrogen bond cleavage corresponding to a formal overall oxidation of H$^-$ to H$^+$, thus keeping the formal oxidation state of the metal; a related, although more complex anodic process — also with liberation, as a proton, of a hydride ligand — has been described by us [33] for the oxidation of *trans*-[FeH(CNMe)(dppe)$_2$]$^+$ to give *trans*-[FeF(CNMe)(dppe)$_2$]$^+$, in the presence of BF$_4$$^-$, through an ECE process. Moreover, we have previously observed [14] anodically-induced single (β-deprotonation processes of aminocarbyne (CNH$_2$) and η^2-vinyl[η^2-C(CH$_2$Ph)CH$_2$] ligands at the metal site *trans*-{ReCl(Ph$_2$PCH$_2$CH$_2$PPh$_2$)$_2$}$^+$ to afford the ligating isocyanide (CNH) and η^2-allene (η^2-CH$_2$=C=CHPh) species.

However, in the current study, most of the above-mentioned anodic processes appear to involve a stepwise deprotonation [31] coupled to the electron-transfer steps, rather than a single H$^+$ loss, as also generally substantiated by the following effects on the cyclic voltammograms:

(i) A decrease of the scan rate results in an increase (Figs. 2 and 3) of the current-function for the waves with a multi-electron transfer character (as indicated by CPE), in agreement with an increase of the number of electrons involved.

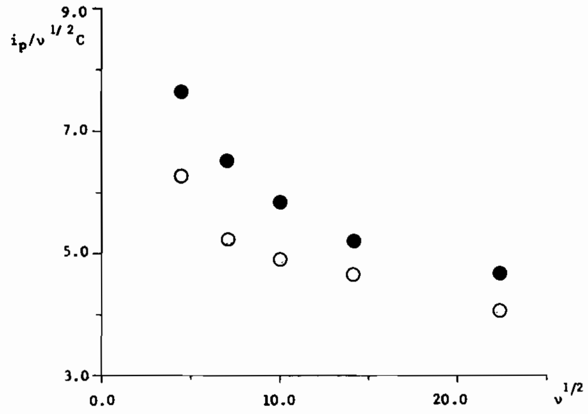

Fig. 3. Effect of addition of pyridine on the current-function for wave(II) of complex **6**, at various scan rates. ○ Without pyridine. ● In the presence of pyridine (1.5:1 molar ratio). $i_p/\nu^{1/2}$ C in mA $s^{1/2}$ mol^{-1} dm^3 $mV^{-1/2}$. $\nu^{1/2}$ in $mV^{1/2}$ $s^{-1/2}$.

(ii) Both a decrease of scan rate (compare Fig. 2(a) with (b) or (c) with (d)) and an increase of temperature (compare Fig. 2(c) with (a) or (d) with (b)) tend to enhance the current-function of wave(s) (II) (with multielectron and associated chemical steps) relative to that of the wave(s) (I) (with a lower number of electrons and protons, not exceeding two), in accord with a promoting effect on the sequence of the chemical steps involved.

(iii) Addition of a base (pyridine) leads to an increase of the current-function for the wave(s) (II) (Fig. 3) by favouring proton extrusion.

Supplementary material

Atomic coordinates, thermal parameters, bond lengths and angles, least-squares planes equations and tables of observed and calculated structure factors are available from author F.B. on request.

Acknowledgements

This work has been partially supported by CNR (Italy)/INIC(Portugal) cooperative research program and by MURST (R.A.M.) and JNICT (A.J.L.P.).

References

1 (a) R. A. Michelin, L. Zanotto, D. Braga, P. Sabatino and R. J. Angelici, *Inorg. Chem., 27* (1988) 93; (b) *27* (1988) 85.

2 (a) H. Motschi and R. J. Angelici, *Organometallics, 1* (1982) 343; (b) L. K. Johnson and R. J. Angelici, *Inorg. Chem., 26* (1987) 973; (c) S. J. Wang and R. J. Angelici, *J. Organomet. Chem., 352* (1988) 157.

3 R. J. Cross, M. F. Davidson and M. Racamara, *J. Chem. Soc., Dalton Trans.,* (1988) 1147.

4 (a) G. Wilkinson, F. G. A. Stone and E. W. Abel (eds.), *Comprehensive Organometallic Chemistry,* Vol. 6, Pergamon, Oxford, 1982; (b) K. H. Dotz, H. Fischer, P. Hofmann, F. R. Kreissl, U. Schubert and K. Weiss, in *Transition Metal Carbene Complexes,* Verlag Chemie, Weinheim, FRG, 1983; (c) K. H. Dotz, in P. S. Bratermann (ed.), *Reactions of Coordinated Ligands,* Vol. 1, Plenum, New York, 1986, Ch. 4; (d) U. Schubert (ed.), *Advances in Metal Carbene Chemistry,* Nato ASI Series, Kluwer, Dordrecht, 1989.

5 W. A. Nugent and J. M. Mayer, *Metal–Ligand Multiple Bonds,* Wiley, New York, 1988.

6 H. Fischer, P. Hofmann, F. R. Kreissl, R. R. Schrock, U. Schubert and K. Weiss, *Carbyne Complexes,* VCH, Weinheim, FRG, 1988.

7 M. K. Lloyd, J. A. McCleverty, J. A. Connor, M. B. Hall, I. H. Hillier, E. M. Jones and G. K. McEwen, *J. Chem. Soc., Dalton Trans.,* (1973) 1743.

8 (a) E. O. Fischer, M. Schluge and J. O. Besenhard, *Angew. Chem., Int. Ed. Engl., 15* (1976) 683; (b) E. O. Fischer, F. J. Gammel, J. O. Besenhard, A. Frank and D. Neugebauer, *J. Organomet. Chem., 191* (1980) 261; (c) E. O. Fischer, D. Wittmann, D. Himmelreich and D. Neugebauer, *Angew. Chem., Int. Ed. Engl., 21* (1982) 444.

9 R. D. Rieke, H.Kojima and K. Öfele, *Angew. Chem., Int. Ed. Engl., 19* (1980) 538.

10 P. J. Krusic, U. Klabunde, C. P. Casey and T. F. Block, *J. Am. Chem. Soc., 98* (1976) 2015.

11 C. P. Casey, L. D. Albin, M. C. Seaman and D. H. Evans, *J. Organomet. Chem., 155* (1978) C37.

12 J.-P. Battioni, D. Lexa, D. Mansuy and J.-M. Savéant, *J. Am. Chem. Soc., 105* (1983) 207.

13 M. Lange and D. Mansuy, *Tetrahedron Lett., 22* (1981) 2561.

14 M. A. N. D. A. Lemos and A. J. L. Pombeiro, *J. Organomet. Chem., 356* (1988) C79.

15 L. Chen and J. A. Davies, *Inorg. Chim. Acta., 175* (1990) 41.

16 R. Bertani, M. Mozzon and R. A. Michelin, *Inorg. Chem., 27* (1988) 2809.

17 A. C. T. North, D. C. Phillips and F. S. Mathews, *Acta Crystallogr., Sect. A, 24* (1968) 351.

18 *International Tables for X-ray Crystallography,* Vol. IV, Kynoch Press, Birmingham, UK, 1974 (present distributor, Kluwer, Dordrecht).

19 G. M. Sheldrick, *SHELX,* a computer program for crystal structure determination, University of Cambridge, UK, 1976.

20 C. K. Johnson, *ORTEP, Rep. ORNL-5138,* Oak Ridge National Laboratory, TN, 1970.

21 M. Nardelli, *Comput. Chem., 7* (1983) 95.

22 L. Zanotto, R. Bertani and R. A. Michelin, *Inorg. Chem., 29* (1990) 3265.

23 L. J. Manoilovic-Muir and K. W. Muir, *Inorg. Chim. Acta, 10* (1974) 47.

24 R. Bardi and A. M. Piazzesi, *Inorg. Chim. Acta, 47* (1981) 249.

25 U. Schubert, *Coord. Chem. Rev., 55* (1984) 261.

26 *Transition Metal Carbene Complexes,* Verlag Chemie, Weinheim, FRG, 1983, p. 73.

27 (a) R. A. Michelin, R. Bertani, M. Mozzon, G. Bombieri, F. Benetollo and R. J. Angelici, *Organometallics, 10* (1991) 1751; (b) H. T. Dieck, G. Fendesack and C. Munz, *Polyhedron, 10* (1991) 255.

28 V. D. Khasnis, M. Lattman and U. Siriwardane, *Inorg. Chem., 28* (1989) 681.

29 T. Shono, *Electroorganic Chemistry as a New Tool in Organic Synthesis,* Springer, Berlin, 1984, Sections 2.3 and 2.6, and refs. therein.

30 F. R. Keene, D. J. Salmon and T. J. Meyer, *J. Am. Chem. Soc., 98* (1976) 1884, and references therein.

31 (a) L. Chen, J. A. Davies and R. Staples, *Inorg. Chim. Acta, 163* (1989) 11; (b) Y. A. Davies, V. Uma and J. G. Mierzwiak, *J. Electroanal. Chem., 196* (1985) 329, and refs. therein.

32 C. K. Mann, *Anal. Chem., 36* (1964) 2424.

33 M. A. N. D. A. Lemos and A. J. L. Pombeiro, *J. Organomet. Chem., 332* (1987) C17.